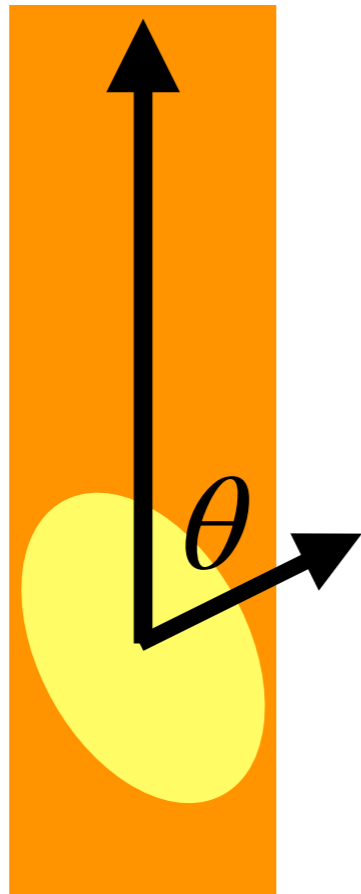


# **Cosmology Dependence of the Transition Mass of Dark Halo Spins**

**Jounghun Lee (Seoul Nat'l Univ.)**

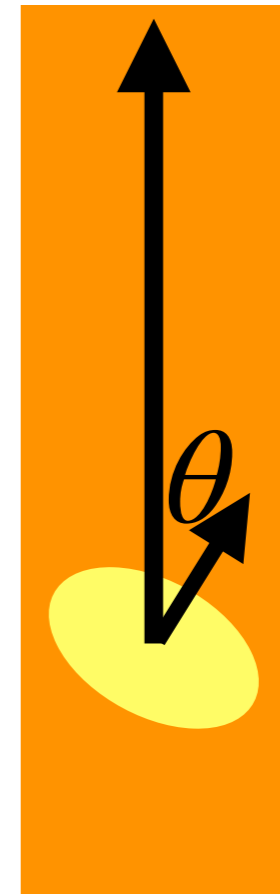
- Lee & Libeskind (ApJ, 2020, 902, 22)
- Lee et al. (ApJ, 2021, 922, 6)
- Lee, Moon, & Yoon (submitted to ApJ, arXiv:2111.13831)

# Halo Spin Transition (HST)



If  $M > M_t$ , then

$$\langle \cos \theta \rangle < 0.5$$



If  $M \leq M_t$ , then

$$\langle \cos \theta \rangle \geq 0.5$$

# Previous Results

- Numerically, the occurrence of HST confirmed.
  - Sensitive dependence of  $M_t$  on how the filaments are identified (e.g., Kraljic et al. 2020).
  - Its occurrence in the sheet environments (e.g., Lee et al. 2020)
- Observationally, a weak signal of the morphology-dependent transition (e.g., Tempel & Libeskind 2013).
- Theoretically, no consensus established.
  - It should be closely linked with the evolution of the halo angular momentum in the cosmic web (Codis et al. 2015).

# Directions of Improvements

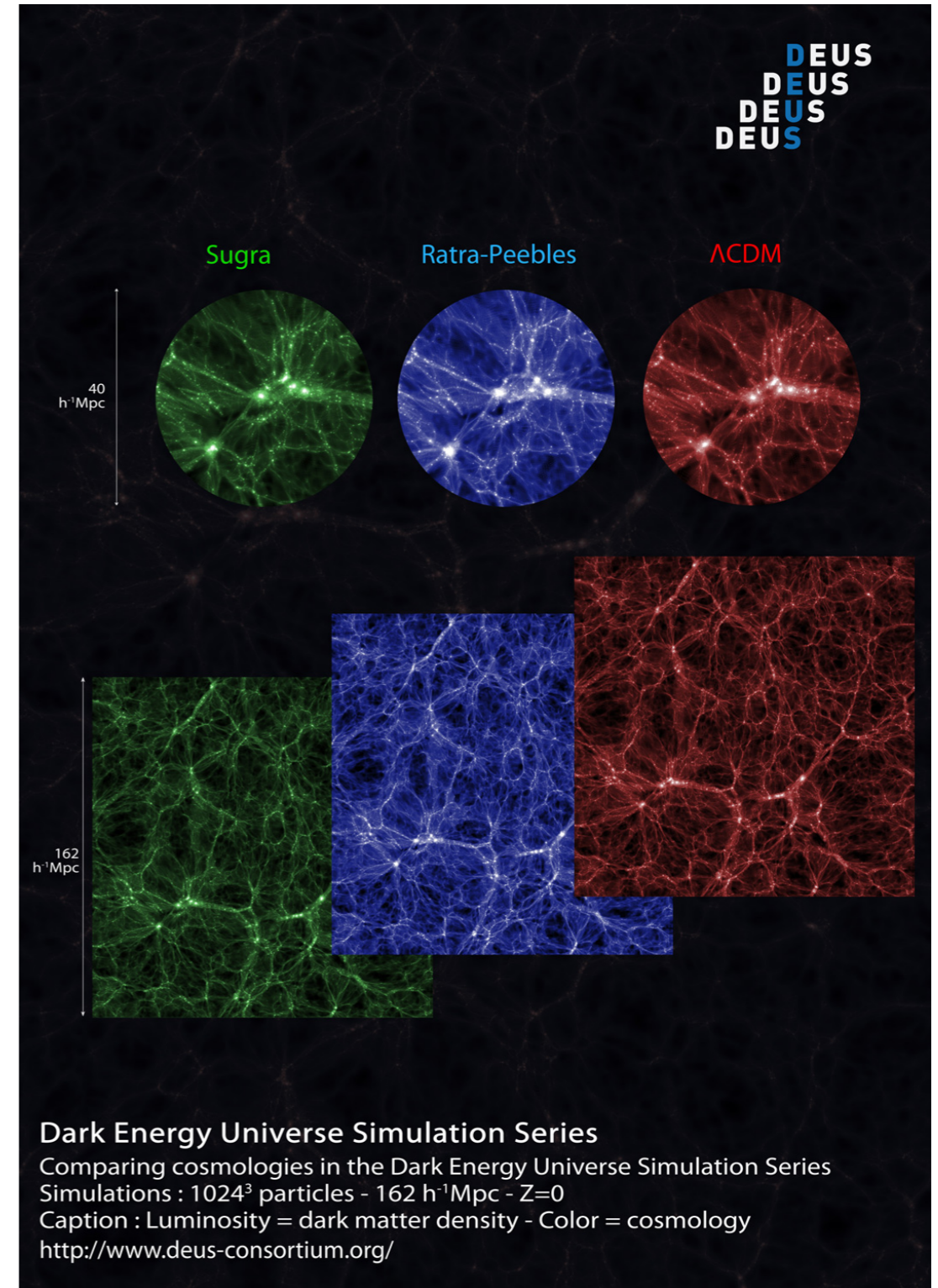
- Considering all of 3 tidal principal directions.
- Finding a more rigorous definition of  $M_t$
- Testing  $M_t$  as a cosmological diagnostics.
- Exploring the galaxy stellar spin transitions.

# Simulation Data

LARGE SET OF UNIVERSE VOLUMES (+ 25 SIMULATIONS)

HIGH SPATIAL RESOLUTION AND MASS:  $2.5 h^{-1} \text{ kpc}$  to  $10.4 h^{-1} \text{ Gpc}$ ,  $2.5 \cdot 10^8 h^{-1} M_{\odot}$  to  $10^{16} h^{-1} M_{\odot}$   
INITIAL REDSHIFT DEEP IN LINEAR REGIME

Box Size	Force Resolution	Mass Resolution	Number of Particles	Initial Redshift	Cosmological Models	Supercomputer (Nb of Proc)
$162 h^{-1} \text{ Mpc}$	$2.5 h^{-1} \text{ kpc}$	$\sim 2 \cdot 10^9 h^{-1} M_{\odot}$	$512^3$	$\sim 90$	$\Lambda\text{CDM}$ , SUCDM, RPCDM	Titane (64)
$162 h^{-1} \text{ Mpc}$	$2.5 h^{-1} \text{ kpc}$	$\sim 2.5 \cdot 10^8 h^{-1} M_{\odot}$	$1024^3$	$\sim 130$	$\Lambda\text{CDM}$ , SUCDM, RPCDM	Blue Gene/P(4096)
$648 h^{-1} \text{ Mpc}$	$20 h^{-1} \text{ kpc}$	$\sim 1.5 \cdot 10^{11} h^{-1} M_{\odot}$	$512^3$	$\sim 55$	$\Lambda\text{CDM}$ , SUCDM, RPCDM	-
$648 h^{-1} \text{ Mpc}$	$10 h^{-1} \text{ kpc}$	$\sim 1.75 \cdot 10^{10} h^{-1} M_{\odot}$	$1024^3$	$\sim 90$	$\Lambda\text{CDM}$ , SUCDM, RPCDM	Blue Gene/P(4096)
$648 h^{-1} \text{ Mpc}$	$5 h^{-1} \text{ kpc}$	$\sim 2 \cdot 10^9 h^{-1} M_{\odot}$	$2048^3$	$\sim 90$	$\Lambda\text{CDM}$ , RPCDM	Blue Gene/P(32768)
$1296 h^{-1} \text{ Mpc}$	$40 h^{-1} \text{ kpc}$	$\sim 1 \cdot 10^{12} h^{-1} M_{\odot}$	$512^3$	$\sim 40$	$\Lambda\text{CDM}$ , SUCDM, RPCDM	-
$2592 h^{-1} \text{ Mpc}$	$40 h^{-1} \text{ kpc}$	$\sim 1 \cdot 10^{12} h^{-1} M_{\odot}$	$1024^3$	$\sim 55$	$\Lambda\text{CDM}$ , SUCDM, RPCDM	Blue Gene/P(4096)
$2592 h^{-1} \text{ Mpc}$	$20 h^{-1} \text{ kpc}$	$\sim 1.5 \cdot 10^{11} h^{-1} M_{\odot}$	$2048^3$	$\sim 55$	$\Lambda\text{CDM}$ , RPCDM	Blue Gene/P(24576)
$5184 h^{-1} \text{ Mpc}$	$40 h^{-1} \text{ kpc}$	$\sim 1 \cdot 10^{12} h^{-1} M_{\odot}$	$2048^3$	$\sim 40$	$\Lambda\text{CDM}$ , RPCDM	Blue Gene/P(24576)
$10368 h^{-1} \text{ Mpc}$	$40 h^{-1} \text{ kpc}$	$\sim 1 \cdot 10^{12} h^{-1} M_{\odot}$	$4096^3$	$\sim 40$	$\Lambda\text{CDM}$	Curie Fat Nodes (9728)



# Cosmological Models

## Initial Conditions and the Particle Mass Resolution

Model	$\Omega_m$	h	$\sigma_8$	$w_0$	$w_a$	$m_p$ ( $10^9 h^{-1} M_\odot$ )
$\Lambda$ CDM	0.257	0.72	0.80	-1.0	0.0	2.3
wCDM	0.275	0.72	0.852	-1.2	0.0	2.4
RPCDM	0.230	0.72	-0.66	-0.87	0.08	2.0

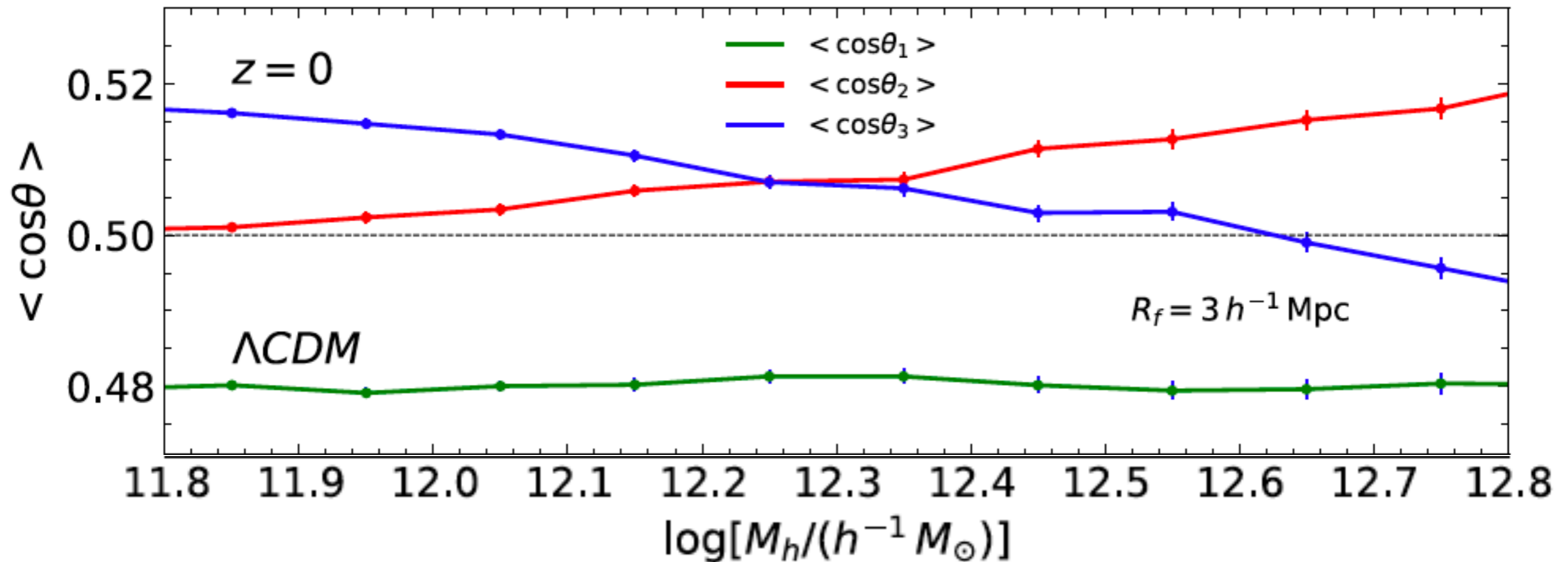
Lee & Libeskind 2020, ApJ, 902, 22

- wCDM: a phantom DE model with negative kinetic energy.
- RPCDM: a quintessence model with Ratra-Peebles scalar field dark energy.
- All of the three models satisfy the same WMAP7 constraints.

# Calculations

- Constructing the tidal fields smoothed on the scale  $R_f$ :
  - Finding three eigenvectors,  $\{\hat{\mathbf{e}}_1, \hat{\mathbf{e}}_2, \hat{\mathbf{e}}_3\}$ , at the positions of the selected halos with 300 or more particles
  - Calculating the cosines of the angles between the halo spin axis,  $\hat{\mathbf{j}}$ , and each of  $\{\hat{\mathbf{e}}_1, \hat{\mathbf{e}}_2, \hat{\mathbf{e}}_3\}$ :  $\cos\theta_i \equiv |\hat{\mathbf{j}} \cdot \hat{\mathbf{e}}_i|$
  - Ensemble averages,  $\langle \cos\theta_i \rangle$ , as a function of the halo mass  $M_h$





- Transition of the preferential direction of  $\hat{\mathbf{j}}$  from  $\hat{\mathbf{e}}_2$  to  $\hat{\mathbf{e}}_3$ , as  $M_h$  decreases.
- The preferential direction of  $\hat{\mathbf{j}}$  being perpendicular to  $\hat{\mathbf{e}}_1$ , regardless of  $M_h$ .

# A New Definition of $M_t$

- Setting up a null hypothesis,  $H_0$  :

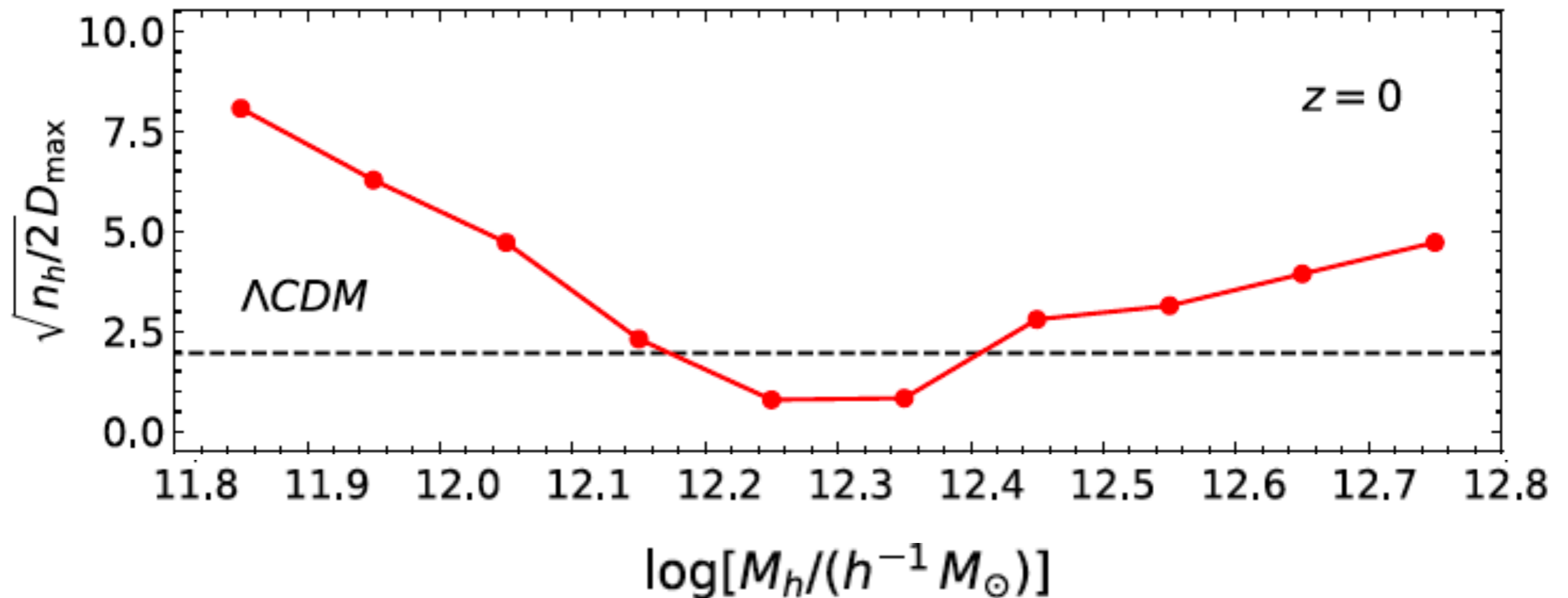
$$p(\cos \theta_2) \sim p(\cos \theta_3)$$

- Performing a KS test of  $H_0$  :
  - Finding the mass bin at which the KS test rejects  $H_0$  at the C.L. below 99.9%.
  - Defining the bin as the spin transition zone,  $M_t$

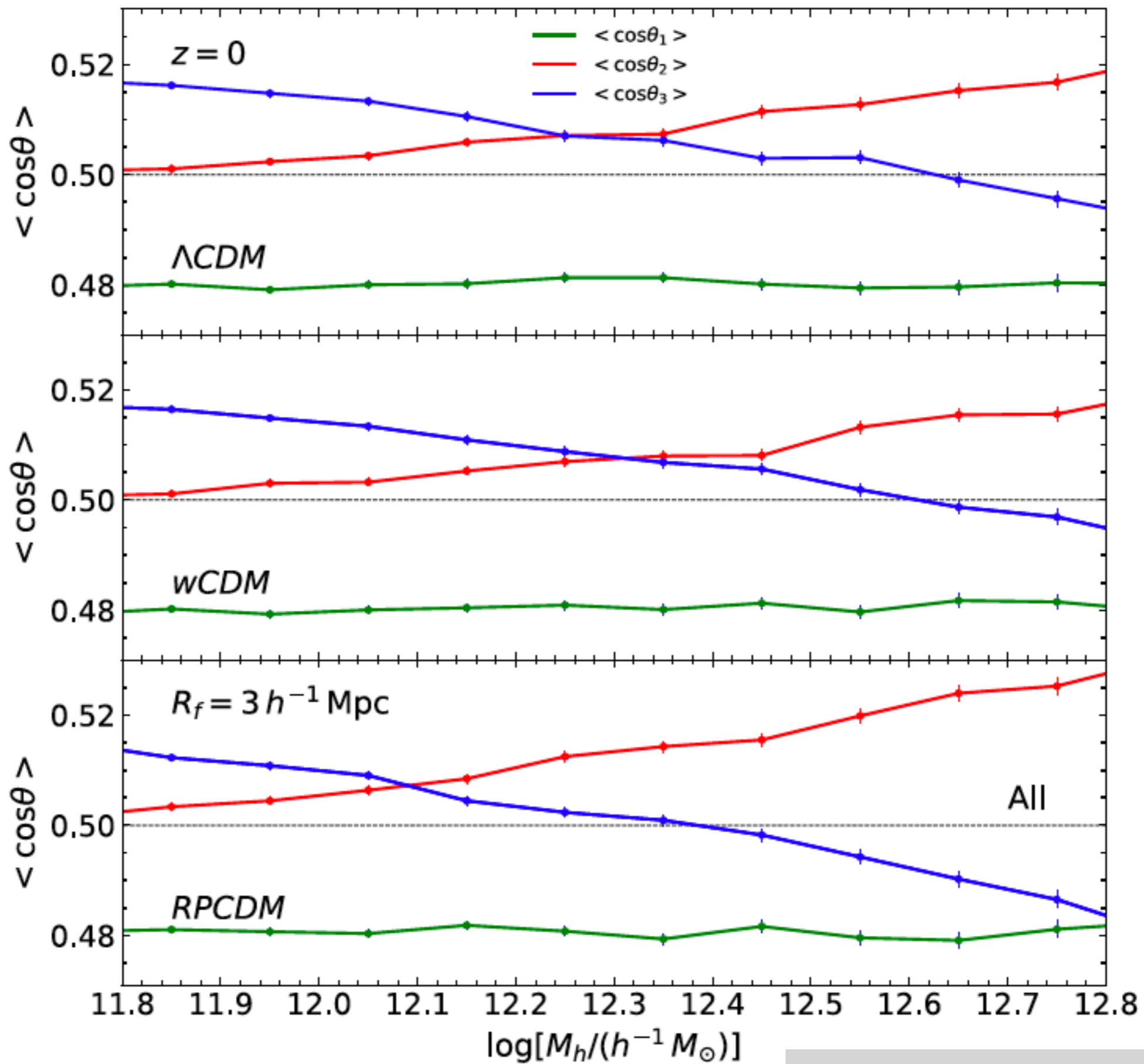
$$D_{\max} \equiv \text{Max}_{\theta} \{ | P(\cos \theta \geq \cos \theta_2) - P(\cos \theta \geq \cos \theta_3) | \}$$

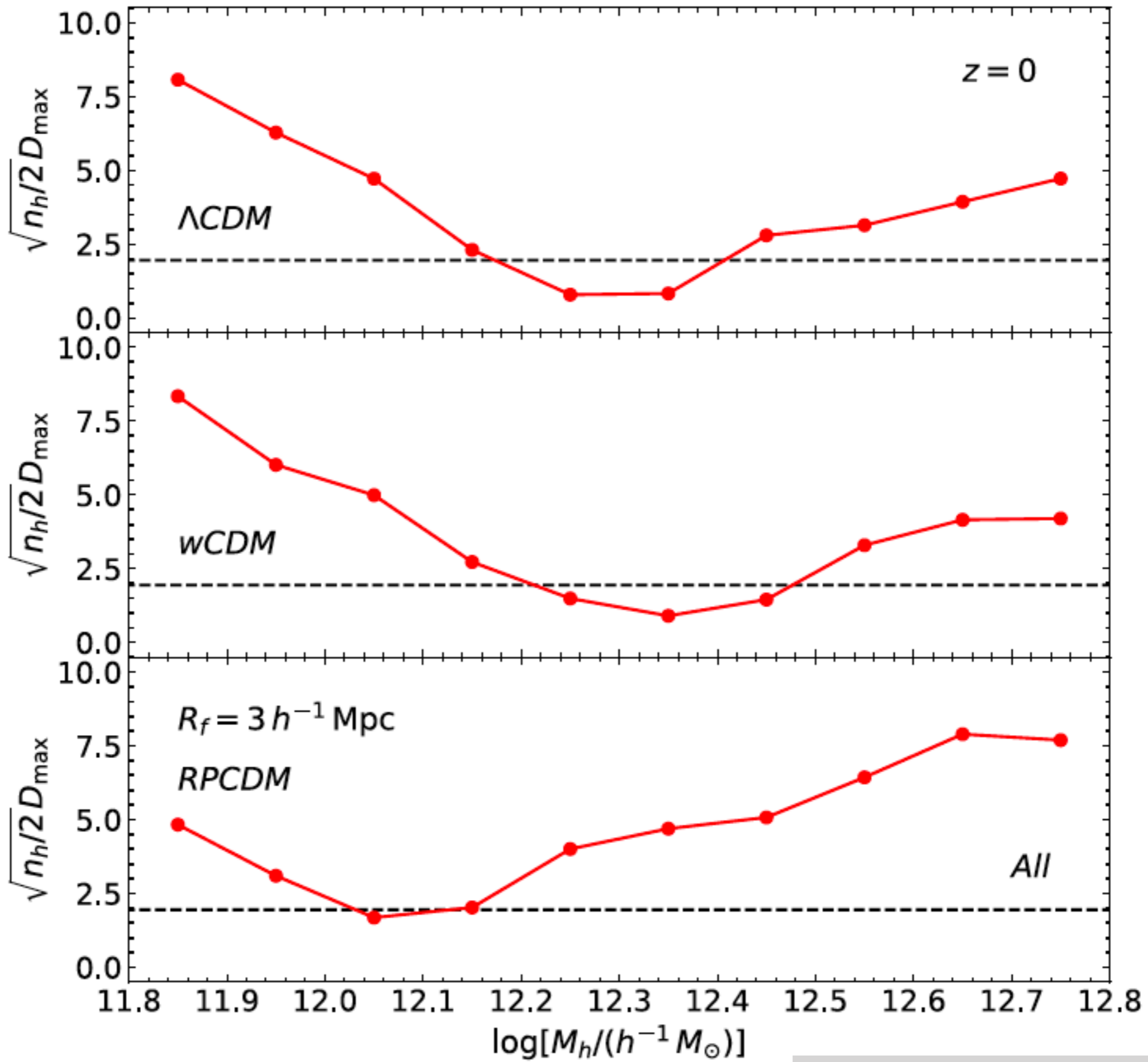
$$\sqrt{\frac{n_h}{2}} D_{\max} \leq 1.99 \quad \leftrightarrow \quad C.L. \leq 99.9\%$$

Lee & Libeskind 2020, ApJ, 902, 22

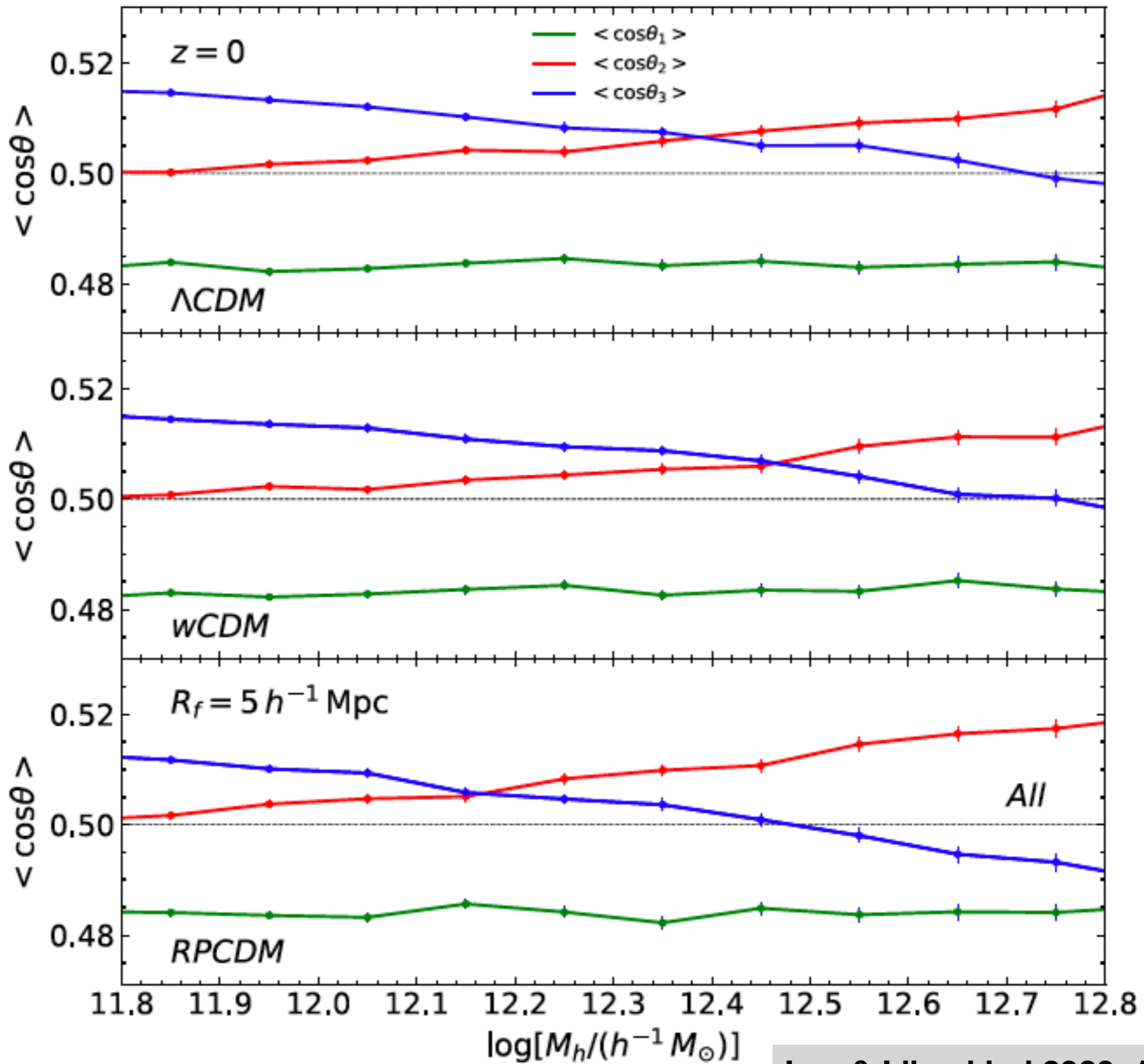


# Variation of $M_t$ with Cosmology

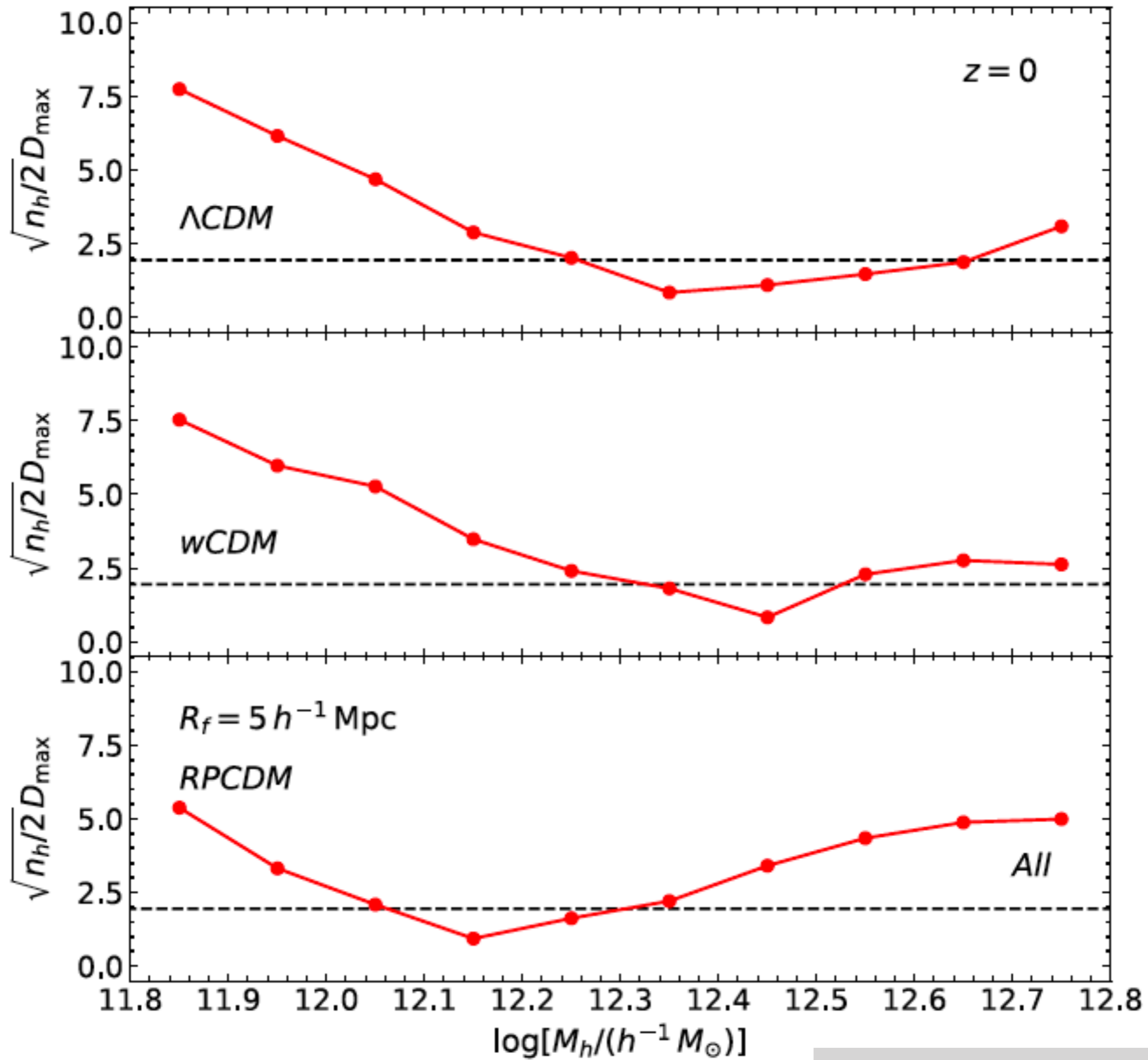




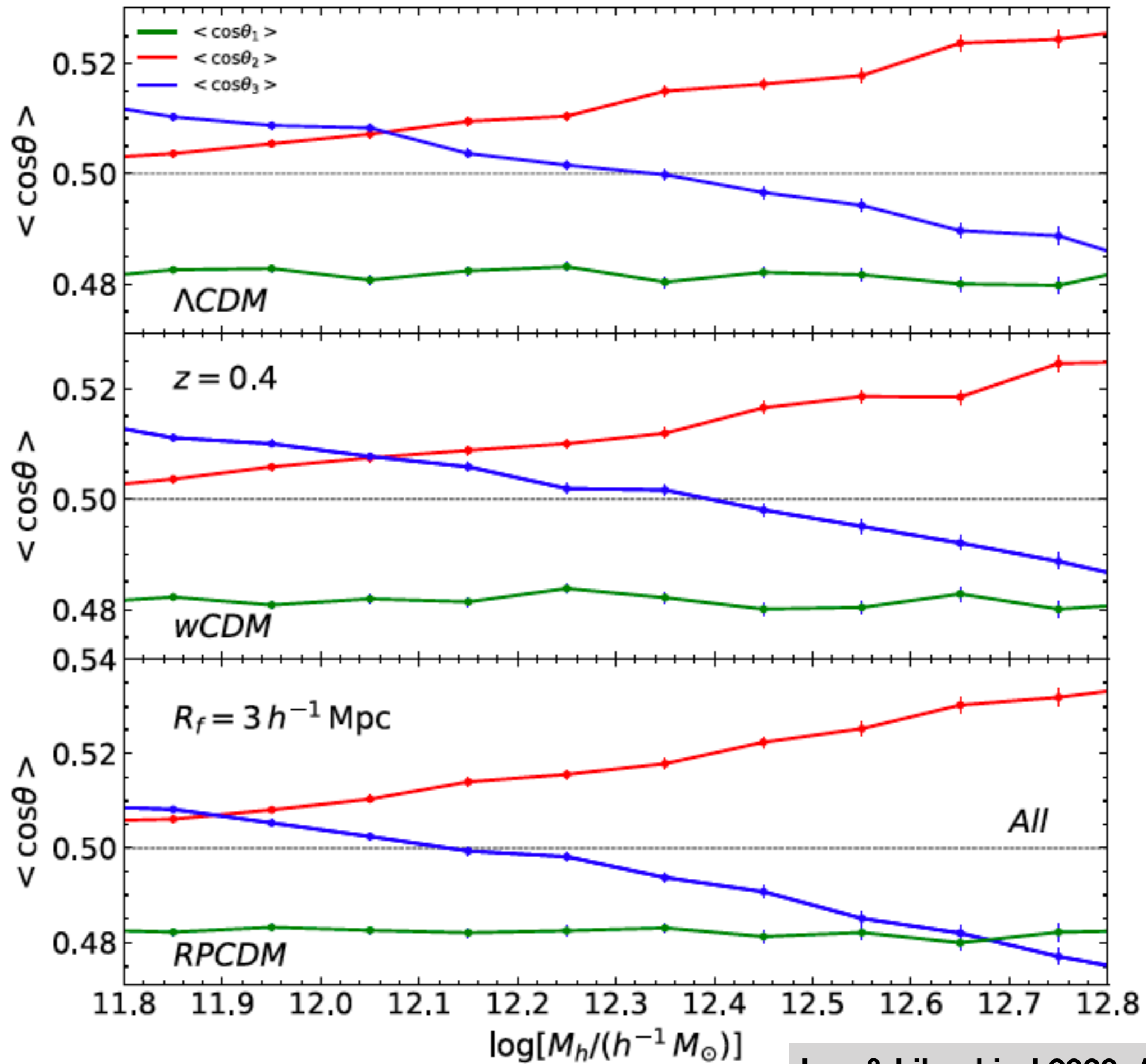
# Variation of $M_t$ with Smoothing Scale

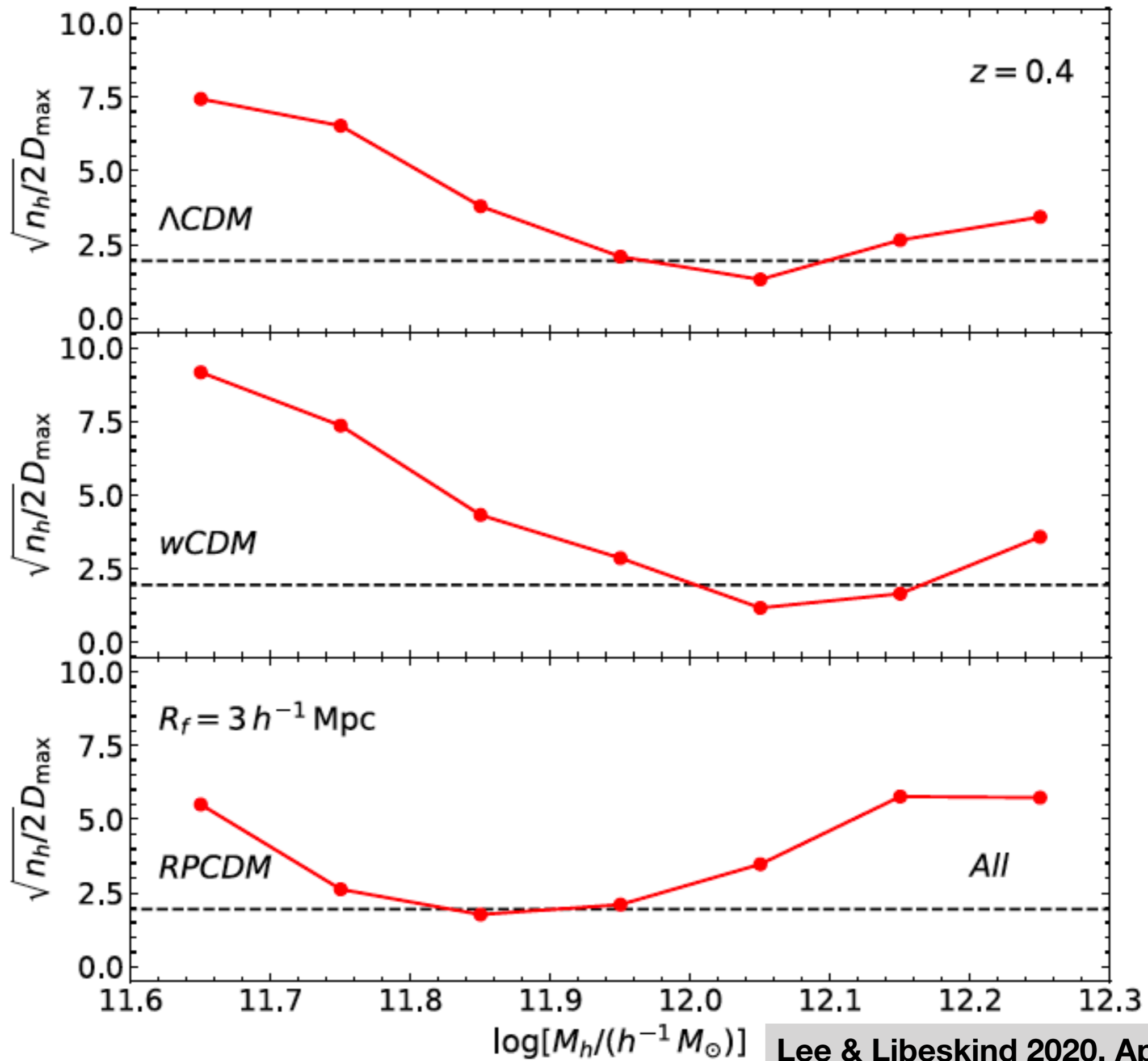




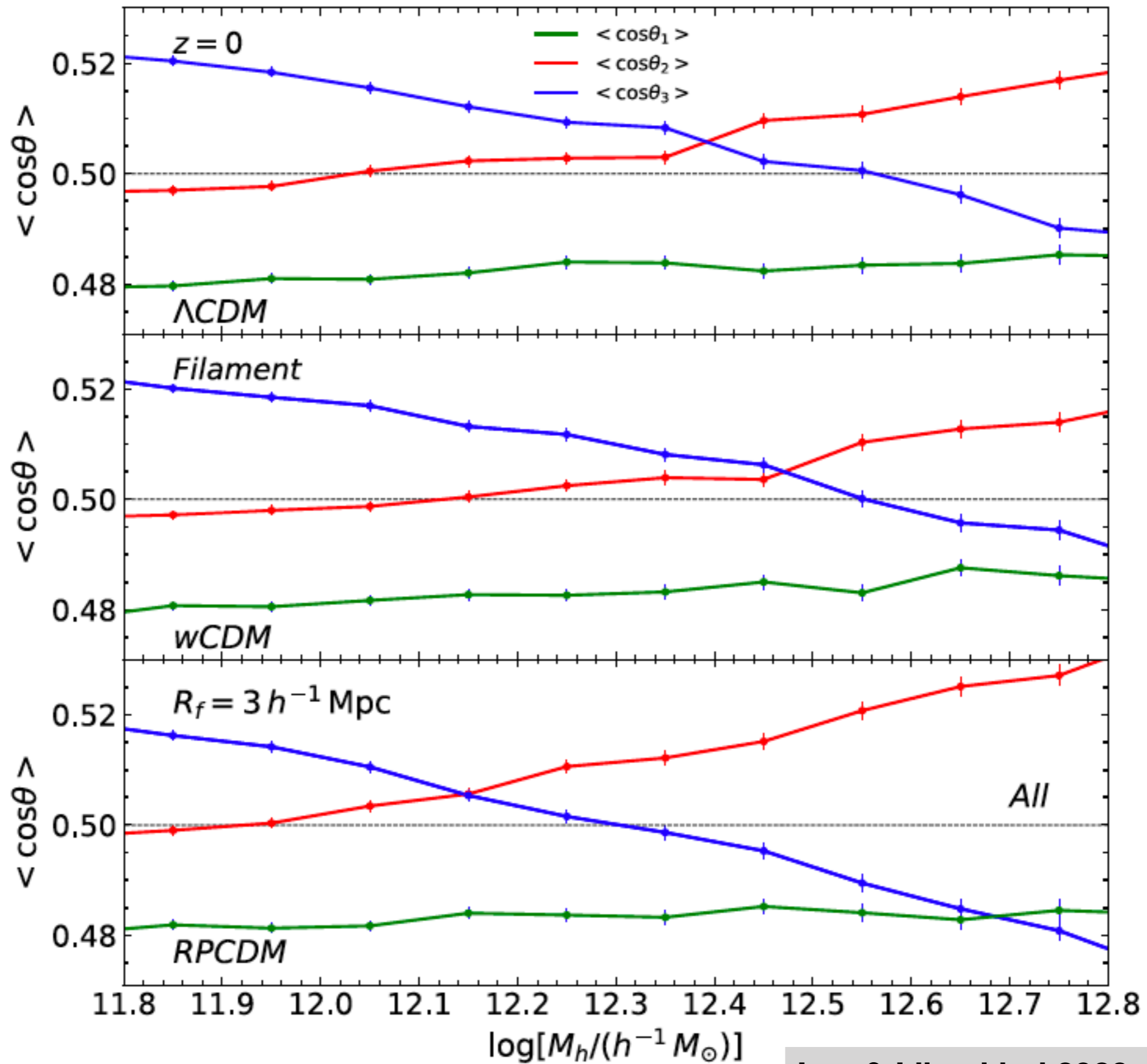


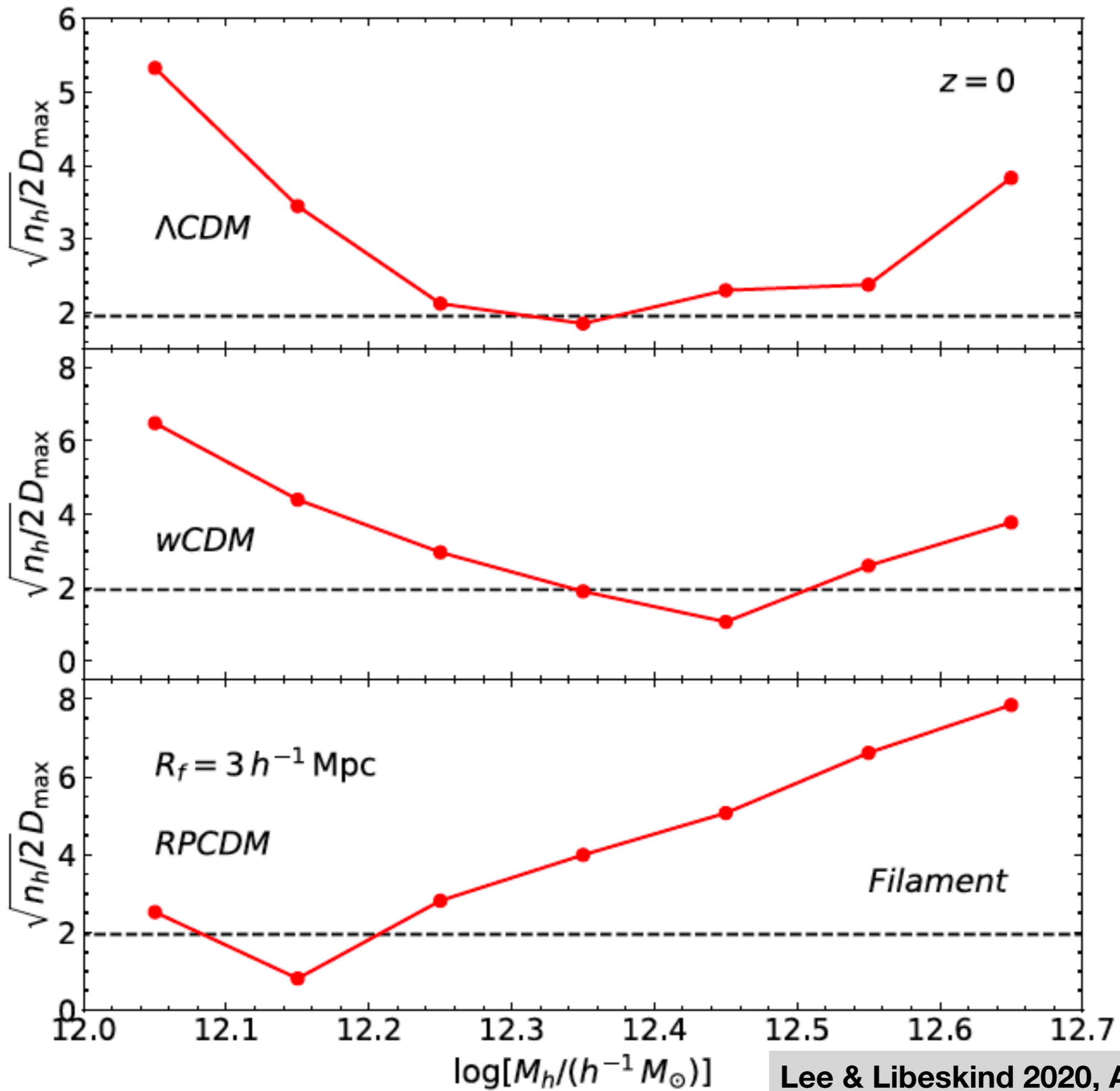
# Variation of $M_t$ with Redshifts

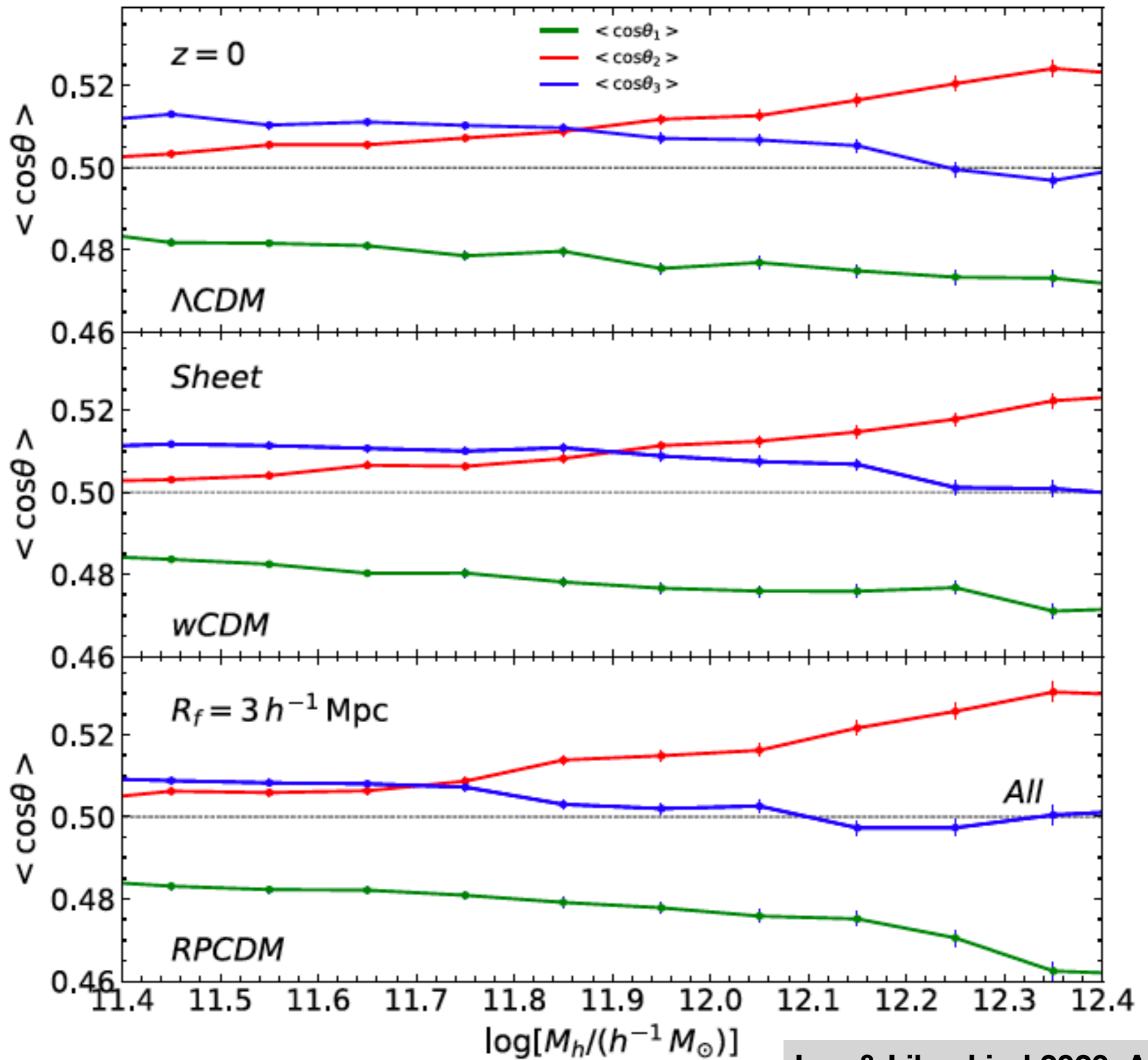




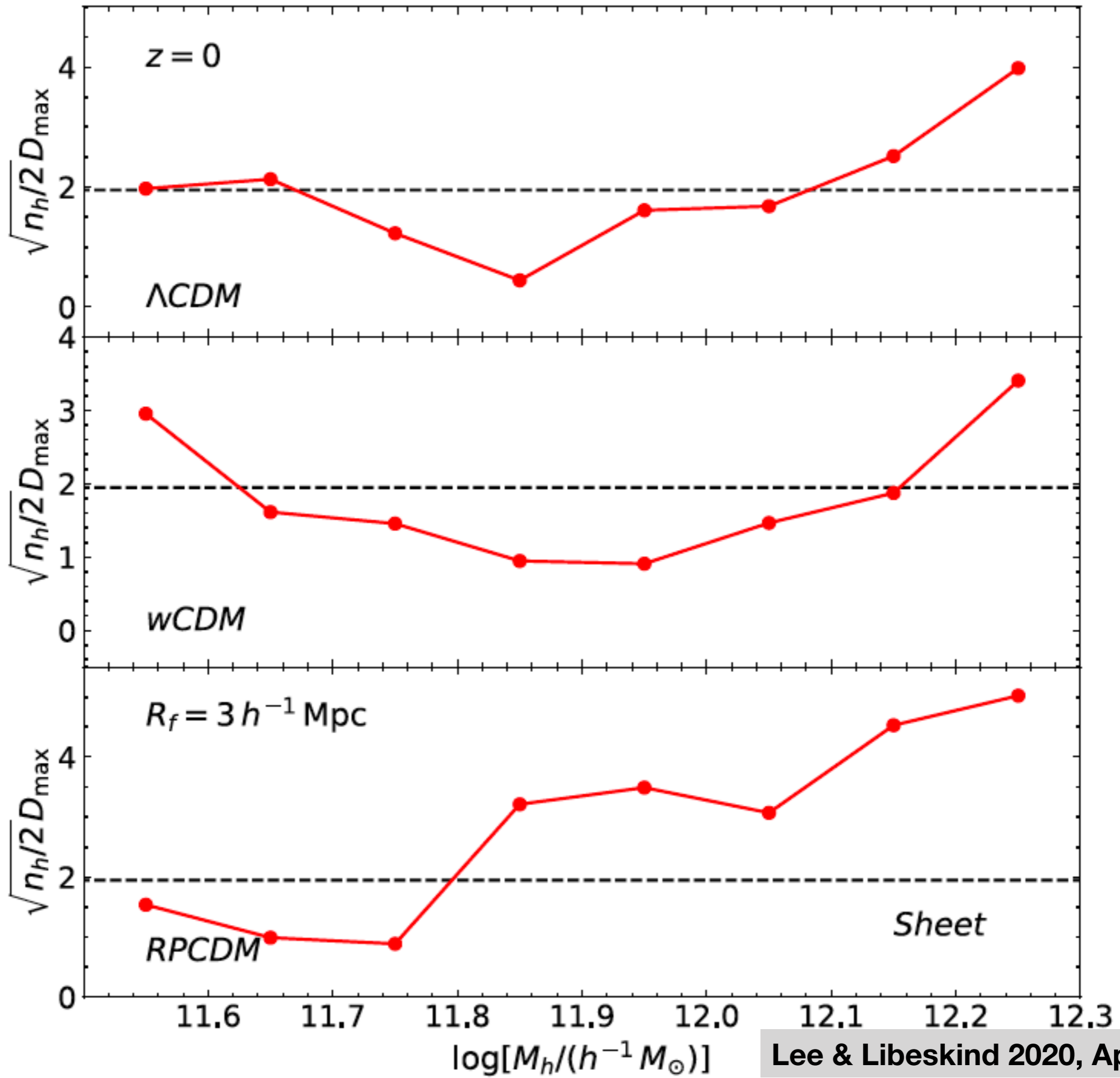
# Variation of $M_t$ with Web Type







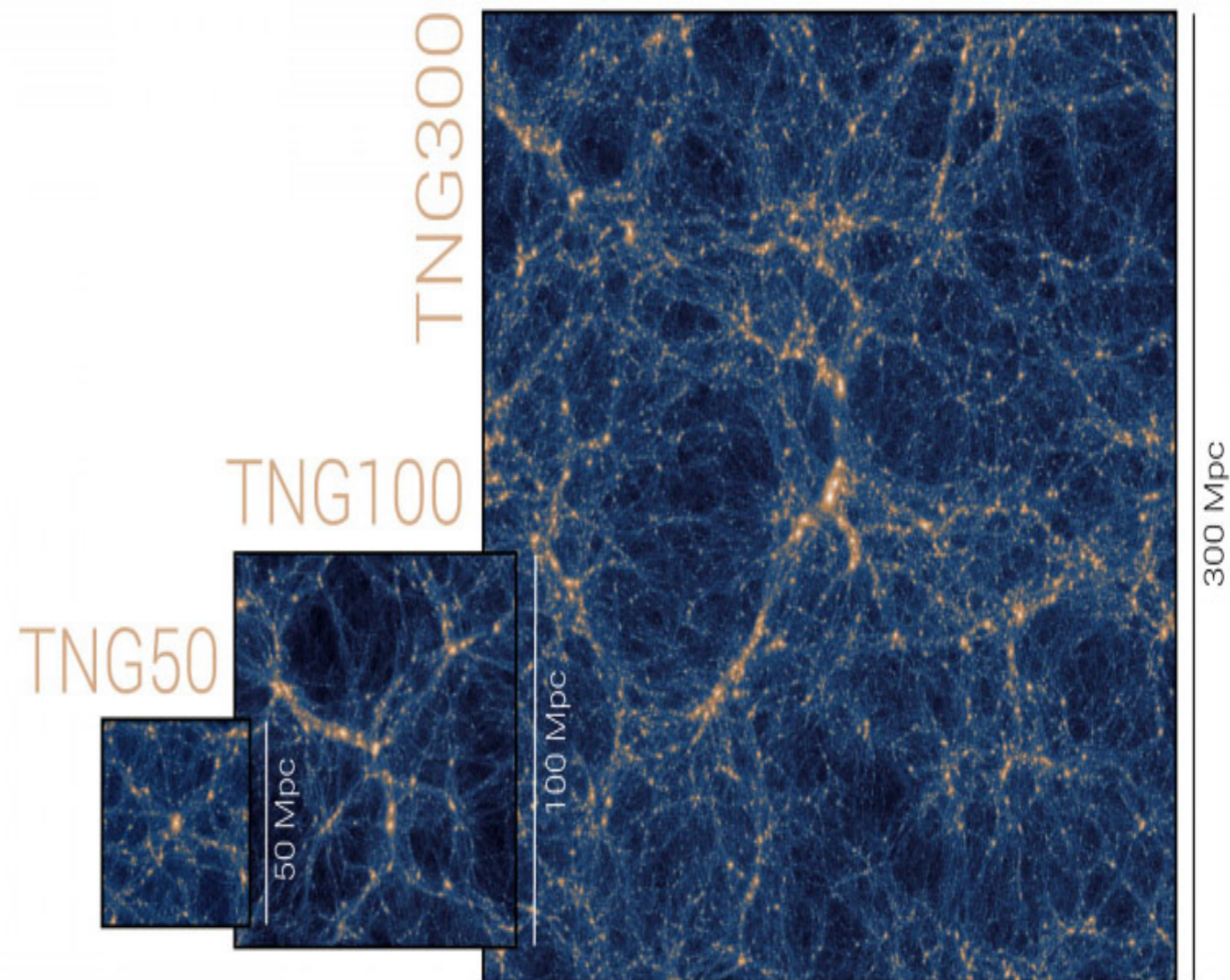


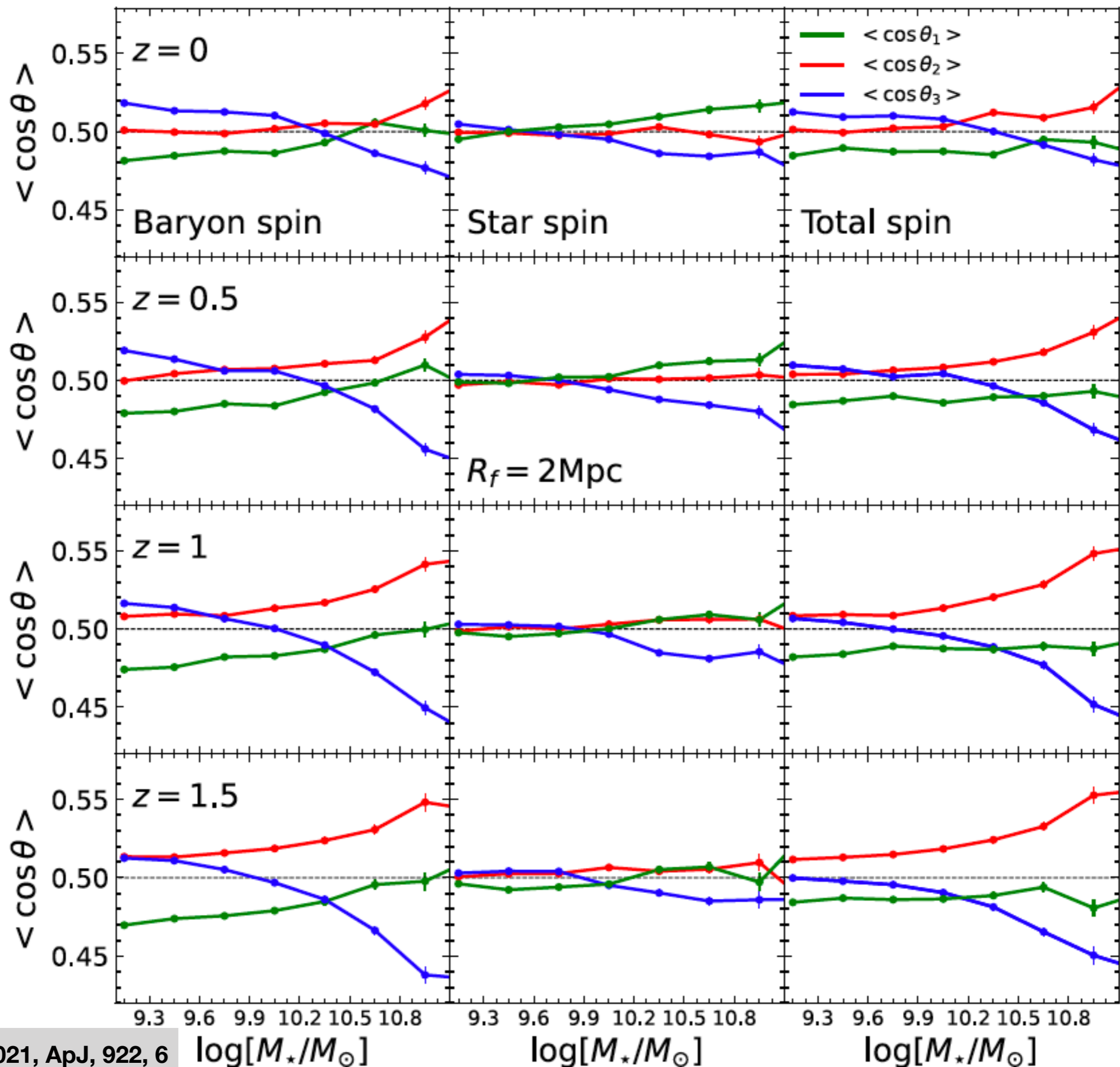


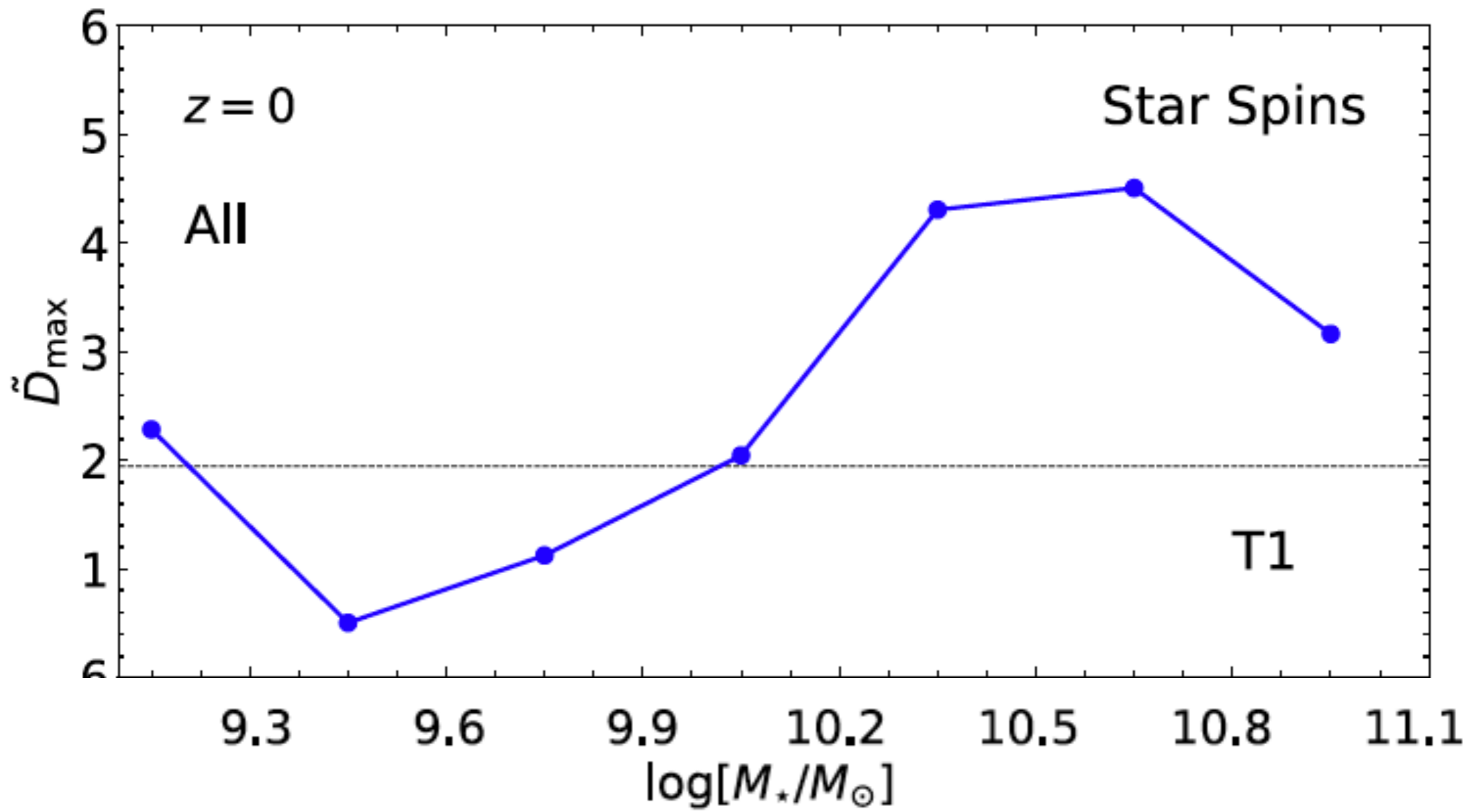
**A Different Type of  
Transition of the Galaxy  
Stellar Spins**

# Hydrodynamic Simulation Dataset

- IllustrisTNG 300-1
  - Full baryon physics
  - Planck cosmology
  - $m_{gas} = 1.1 \times 10^7 M_{\odot}$
  - $L_{box} = 302 \text{ Mpc}$
  - Subhalos with 300 or more stellar cells







# Summary

- The halo spin directions transit between **the tidal intermediate and minor principal axes** in the spin transition zone,  $M_t$ 
  - A new algorithm based on the KS test is developed to rigorously determine  $M_t$ .
- The range of  $M_t$  varies with redshift, smoothing scale, web-type and background cosmology as well.
  - It becomes narrower at higher redshifts, on the smaller scales, in the filamentary environments, and for dynamical DE models.
  - It can distinguish among  $\Lambda$ CDM,  $w$ CDM and RPCDM.
- The galaxy stellar spins transit between **the tidal major and minor principal directions**.

# Discussion

- The halo spin transition may be related to the nonlinear growth of the tidal fields:
  - Retarded nonlinear growth of the tidal fields can induce smaller values of  $M_t$ .
- The galaxy spin transition might be induced by anisotropic occurrence of discharge of stellar materials by the galactic winds (Lee et al. 2021, arXiv:2111.13831)